Risk Averse Model Predictive Control of Bioreactors

Satyajeet Bhonsale * **Maurits Descamps** *
Mihaela Iuliana Sbarciog * **Pantelis Sopasakis** **
Jan Van Impe *

* *BioTeC+, Department of Chemical Engineering, Technology Campus Ghent, KU Leuven, Gebroeders de Smetstraat 1, 9000 Ghent, Belgium*
** *Centre for Intelligent Autonomous Manufacturing Systems, School of Electronics, Electrical Engineering and Computer Science, Queen's University Belfast, Northern Ireland*

Abstract: Uncertainty is inherent in bioprocess modelling and control. Typically, uncertainties are handled using either the stochastic approach or the robust approach. Recently, the risk-averse approach, i.e., an interpolation between the stochastic and worst-case robust approach is gaining popularity. Risk-averse formulations are very useful in avoiding conservative solutions while still handling high-effect, low-probability events. In the bioreactor case considered in this paper, one such high effect low probability event is wash off caused by high feed rate or low inlet substrate concentration. A risk-averse, risk-constrained model predictive control formulation is proposed in this paper. The dynamic optimisation problem to be solved at every measurement instance is formulated using AV@R type risk objective. Similarly, probabilistic chance constraints are approximated by an AV@R-type risk constraints. The problem is then solved using the conic duality of the risk measure and an epigraphical decomposition of the nested multistage problem.

Keywords: uncertainty; risk-averse optimisation; model predictive control; bioreactor control

1. INTRODUCTION

Fed-batch bio-reactors are the workhorses of the biochemical industry. Their applications range from fermentation to produce sweeteners (Joseph et al., 2019), proteins (Cereghino et al., 2002; Çalık et al., 2010), alcohol (Alfenore et al., 2004), etc to waste-water treatment (Lauwers et al., 2013). In a fed-batch reactor operation, the reactor is first inoculated with the bacteria or yeast culture. Unlike batch operation, the substrate on which the cells grow is fed continuously to the reactor. However, unlike the continuous operation, the fermentation (or bioconversion) products are removed from the reactor only at the end of the batch. The rate at which the substrate is fed to the bioreactor can be used to control the operation, stability, and productivity of the bioreactors (Bastin, 1990). Typically, offline dynamic optimisation strategies are utilised to determine the feeding profile of for the bioreactor to optimise a desired objective (Bhonsale et al., 2019; Pushpavanam et al., 1999). However, in absence of any feedback from measurements, application of the feeding profile obtained from offline dynamic optimisation can lead to erroneous outcomes due to plant-model mismatch, measurements uncertainty, and the existence of unknown disturbances. Such a feedback can be incorporated into the control strategy using model predictive control (MPC).

In MPC, a discrete-time finite-horizon problem is solved to optimise a desired objective. While the entire optimal sequence of control actions is obtained, only the first action is applied to the system till a new measurement is available. Once a new measurement is available, the optimal control problem is solved again with the new measurement as the initial condition. Traditionally, MPC was developed for setpoint tracking. Recently however, economic MPC in which an economic cost function (e.g., production, costs) is optimised rather than the deviation from setpoint has been developed (Angeli et al., 2012). A variety of studies utilise MPC for control and optimisation of bioreactors (Ashoori et al., 2009; Chang et al., 2016; Nimmegeers et al., 2021).

Although the feedback incorporated in MPC can handle a small plant-model mismatch, uncertainties in the model can drastically affect the accuracy, efficiency, stability of the process, or even lead to violations of the state constraints. Two main approaches exist to handle uncertainties in an MPC context. In the *robust approach*, the worst-case realisation of the (random) cost function is optimised (Rawlings et al., 2020). Such an approach does not utilise any information about the distribution of the uncertainties, i.e., an non-informative prior is assumed. However, the occurrence of these worst-case extreme events is in most cases unlikely. Thus, the control profile obtained from a robust approach tends to be conservative. In the *stochastic approach*, the expectation of the objective obtained by propagating the distribution of the uncertainty through the process model is optimised (Mesbah, 2016). This approach requires the distribution of the uncertainties to be known explicitly. Often, these distributions are assumed to be normal, or estimated from data. However, accuracy of such estimates and assumptions cannot be guaranteed.

Most often, only inexact information about the uncertainty distribution is available. *Risk measures* allow the incorporation of this *uncertainty on the uncertainty* in an optimisation or MPC framework (Herceg, 2019). This allows the interpolation between the two approaches used to account for uncertainties, i.e., the worst-case robust approach and expectation based stochastic approach. The formulation of a risk-averse MPC problem leads to optimisation of the expectation of the objective for the worst-case probability distribution. This makes risk-averse optimisation a subset of *distributionally robust optimisation* (Rahimian and Mehrotra, 2019).

In this paper, a risk-averse MPC formulation is proposed for the optimisation of bioreactors. As it is also desirable to account for the uncertainties in the constraints that are imposed on the process system, risk constraints are formulated following Sopasakis et al. (2019). These risk constraints are used as convex approximations of the chance constraints (Nemirovski and Shapiro, 2007) to improve the computational efficiency. The optimisation problem is rendered tractable by utilising the conic representation of coherent risk measures (Sopasakis et al., 2019).

The paper is organised as follows: first the fed-batch bioreactor model is introduced along with the dynamic optimisation problem that needs to be solved. Then the concepts of scenario trees, risk measures, and risk averse, risk constrained optimisation are introduced. Then the tractable reformulation of the problem is described. The last section discusses the results obtained from the risk averse MPC.

Notation

In this paper, $\mathbb{N}_{[k_1,k_2]}$ denotes the integers between k_1 and k_2. The transpose of the a matrix A is given by $A^\top$. The dual cone $\mathcal{K}^*$ of a closed convex cone $\mathcal{K}$ is the set $\mathcal{K}^* = \{y \in \mathbb{R}^n \mid y^\top x \geq 0, \forall x \in \mathcal{K}\}$. A conic inequality of form $x \preccurlyeq_{\mathcal{K}} y$ is interpreted as $x - y \in \mathcal{K}$.

2. NUMERICAL METHODS AND BACKGROUND

2.1 Dynamic Optimisation of fed-batch bioreactor

For a yeast or bacteria which consumes a substrate and utilises it to reproduce as well as produce a product, the macroscopic mass balance leads to the following set of ordinary differential equations for a fed-batch bioreactor (Srinivasan et al., 2003):

$$\dot{X} = \mu(S)X - \frac{u}{V}X, \tag{1}$$

$$\dot{S} = -\frac{1}{Y_x}\mu(S)X - \frac{1}{Y_p}\nu_{\max}X + \frac{u}{V}(\mathrm{S_{in}} - S), \tag{2}$$

$$\dot{P} = \nu X - \frac{u}{V}P, \tag{3}$$

$$\dot{V} = u, \tag{4}$$

where X is the concentration of biomass, S is the concentration of substrate, P is the concentration of the product, and V is the volume of the mixture. The feed rate is denoted by u and the substrate concentration in the feed is denoted by $\mathrm{S_{in}}$. Y_x and Y_p are the yield coefficients, while $\mu(S)$ and $\nu(S)$ are the reaction kinetics. The substrate uptake kinetics is assumed to be described by Haldane type kinetics described in Eq. (5) while the product formation kinetics is assumed to be constant

$$\mu(S) = \mu_{\max}\frac{S}{K_m + S + \frac{S^2}{K_I}}. \tag{5}$$

The values of the kinetic parameters can be found in Table 1.

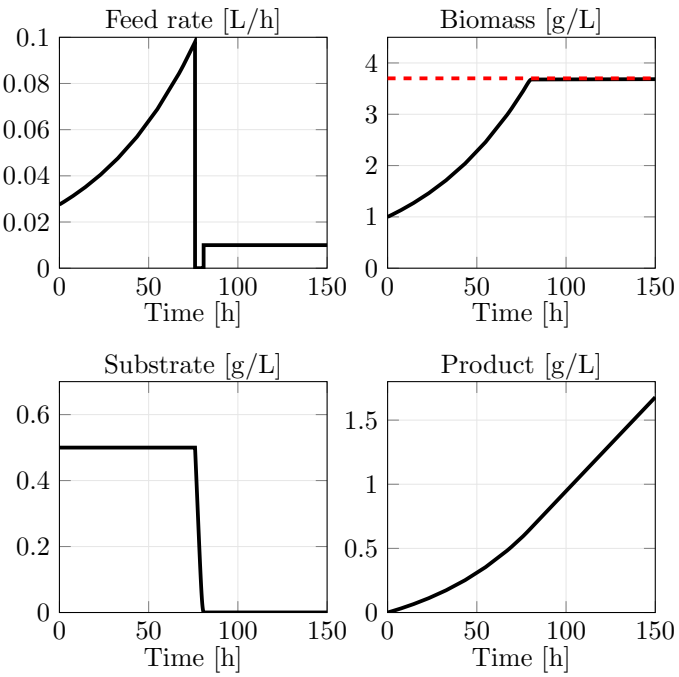

Fig. 1. Analytical optimal trajectories for the fedbatch bioreactor case following Srinivasan et al. (2003)

Table 1. Parameters for the bioreactor model.

Model parameter	Value	Units
$\mu_{\max}$	0.02	1/h
K_m	0.05	g/L
K_i	5	g/L
$\nu_{\max}$	0.004	1/h
Y_x	0.5	g[X]/g[S]
Y_p	1.2	g[P]/g[S]
$\mathrm{S_{in}}$	200	g/L

The objective of the optimisation is to maximise the product concentration at every time instance. The final fermentation time is fixed at 150 h, and the input is constrained between $0\,\mathrm{L/h}$ and $1\,\mathrm{L/h}$. Furthermore, due to limitations in oxygen transfer at high biomass loads, the maximum permissible concentration of biomass within the reactor is $3.7\,\mathrm{g/L}$. For a prediction horizon of N stages, the optimal control problem to be solved at every measurement instance can then be formulated as

$$\underset{\substack{u_0,u_1,\ldots,u_{N-1}\\ x_0,x_1,\ldots,x_N}}{\textbf{minimize}} \quad J \tag{6}$$

$$\text{subject to,} \quad x_{t+1} = f(x_t, u_t) \tag{7}$$

$$X_t \leq 3.7, \qquad \forall t \in \mathbb{N}_{[0,N]} \tag{8}$$

$$0 \leq u_t \leq 1, \qquad \forall t \in \mathbb{N}_{[0,N-1]}\,. \tag{9}$$

Eq. (7) represents the discretised system (in this case using first order Euler method) of differential equations

described in Eq. (1)- Eq. (4) with the subscript t denoting the stage and $x_t = [X_t\ S_t\ P_t\ V_t]$.

The cost function is defined as

$$J = \sum_{t=0}^{N_p-1} x_{t+1}^\top Q x_{t+1} + r(\Delta u_t)^2, \tag{10}$$

where $t \in \mathbb{N}_{[0,N]}$ denotes the discrete time step, $\Delta u_t = u_t - u_{t-1}$ is the difference between consecutive control actions, and

$$Q = \begin{bmatrix} 0 & 0 & 0 & 0 \\ 0 & 0 & 0 & 0 \\ 0 & 0 & -1 & 0 \\ 0 & 0 & 0 & 0 \end{bmatrix} \quad \text{and} \quad r = 0.5. \tag{11}$$

The optimal solution of this specific problem can be computed analytically and leads to the final product concentration of 1.68 g/L. The analytical trajectories are depicted in Figure 1.

For the risk-averse MPC (RAMPC), it will be assumed that only the inlet substrate concentration is uncertain and varies hourly. S_{in} is a random process described by a scenario tree (see Section 2.2). In our simulations we shall assume that S_{in} follows an iid normal distribution, $\mathcal{N}(200, 25)$, as in Lucia and Engell (2013). All other parameters are assumed to be known accurately. Furthermore, the RAMPC will be formulated as a multistage risk-averse optimisation problem using the concept of scenario trees. This approach has already been used for a stochastic MPC in which the expectation of the objective over all the scenarios is optimised (Lucia and Engell, 2013). The concept of scenario trees is introduced next.

2.2 Scenario Tree

To incorporate uncertainty, the state update of the discretized version of model in Eq. (1)- Eq. (4) can be made dependent on the realisation of the random variable as

$$x_{t+1} = f(x_t, u_t, w_t) \qquad \forall t \in \mathbb{N}_{[0,N-1]}\,. \tag{12}$$

Starting from a known initial state, different realisations of the random variable lead to a tree like structure which grows at every stage. An example of scenario tree is depicted in Figure 2. The *nodes* of this tree are assigned a unique index i. The initial state corresponds to the the *root node* and is assigned the index $i = 0$. The nodes at stage $t \in \mathbb{N}_{[0,N]}$ are denoted by $\mathbf{nodes}(t)$. The nodes at the final stage, $\mathbf{nodes}(N)$, are referred to as *leaf nodes*. Variables defined at a specific node get the index of that node as superscript. To describe the relation between different nodes, two functions are defined. The unique *ancestor* of node $i \in \mathbf{nodes}(t)$ for $t \in \mathbb{N}_{[1,N]}$ is denoted by $\mathbf{anc}(i)$ and the set of *children* of $i \in \mathbf{nodes}(t)$ for $t \in \mathbb{N}_{[0,N-1]}$ by $\mathbf{child}(i) \subseteq \mathbf{nodes}(t+1)$. Additionally, all non-leaf nodes are also assigned an input u^i. The generalised system Eq. (12) can now be used to describe each node as

$$x^{i_+} = f(x^i, u^i, w^{i_+}), \tag{13}$$

where $i \in \mathbf{nodes}(t)$, $t \in \mathbb{N}_{[0,N-1]}$ and $i_+ \in \mathbf{child}(i)$. The different w^{i_+} can be seen as all the possible realizations of w_{t+1}. Each paths from the root node to an end-node $i \in \mathbf{nodes}(N)$ is called a *scenario*.

2.3 Risk Measures

Let $\Omega = \{\omega_i\}_{i=1}^n$ be a finite sample space and P a probability measure with $\mathrm{P}[\{\omega_i\}] = \pi_i$, together forming the probability space (Ω, P). The vector $\pi \in \mathbb{R}^n$ is a *probability vector*, which means that all its elements are positive and sum up to one. The set of all possible probability vectors in $\mathbb{R}^n$ is called the *probability simplex* and is denoted by $\mathcal{D}_n$. In what follows, events with a zero probability will have no effect on the calculations, so all π_i will be assumed to be strictly positive. Let Z be a real-valued random variable over (Ω, P), defined as $Z\colon \Omega \to \mathbb{R}$ with $Z(\omega_i) = Z_i$.

A *risk measure* is a function that maps the random variable Z to the extended real line, i.e., $\rho(Z) : \mathbb{R}^n \to \mathbb{R}$. A risk measure is considered to be coherent if it satisfies the following condition:

- Convexity: $\rho(tZ + (1-t)Z') \le t\rho(Z) + (1-t)\rho(Z')$ for all $t \in [0, 1]$.
- Monotonicity: If $Z_i \le Z_i'$ for all $i \in \mathbb{N}_{[1,n]}$, then $\rho(Z) \le \rho(Z')$.
- Translational equivariance: If $a \in \mathbb{R}$, then $\rho(Z + a) = \rho(Z) + a$.
- Positive homogeneity: If $t > 0$, then $\rho(tZ) = t\rho(Z)$.

The expectation operator $\mathbb{E}_\pi[Z] = \pi^\top Z$ is an example of coherent risk measure. A coherent risk measure can be represented in its dual form as

$$\rho[Z] = \max_{\mu \in \mathcal{A}(\pi)} \mathbb{E}_\mu[Z] \tag{14}$$

where $\mathcal{A}(\pi) \subseteq \mathcal{D}_n$ is the *ambiguity set* of the risk measure ρ and is a closed and convex set of probability vectors containing π. The ambiguity set reflects how much uncertainty there is in the probabilistic information. The larger the ambiguity set, the larger the risk will be.

Another common coherent risk measure is the *average value-at-risk* (AV@R). The ambiguity set for AV@R with a parameter α is given by

$$\mathcal{A}_\alpha^{\mathrm{AV@R}} = \left\{ \mu \in \mathbb{R}^n \;\middle|\; \sum_{i=1}^n \mu_i = 1, 0 \le \alpha\mu_i \le \pi_i, i \in \mathbb{N}_{[1,n]} \right\}. \tag{15}$$

The AV@R interpolates between the risk-neutral expectation operator when $\alpha = 1$, and the worst-case maximum when $\alpha = 0$. In this paper, AV@R will be used as the risk measure to formulate the RAMPC problem.

2.4 Risk averse, risk constrained optimal control

Under uncertainty, the objective function becomes a random variable with a realisation on each node of the scenario tree. This realisation at a node i is denoted by J^i. At each stage t, another random variable is defined: $J_t = (J^i)_{i \in \mathbf{nodes}(t)}$. The variable J_t is partitioned into groups based on a shared common ancestor by defining $J^{[i]} = (Z^{i_+})_{i_+ \in \mathbf{child}(i)}$. The risk measure of this random variable on the probability space $\mathbf{child}(i)$ is denoted by $\rho^i : \mathbb{R}^{|\mathbf{child}(i)|} \to \mathbb{R}$. Then, a *conditional risk mapping* $\rho_{|t} : \mathbb{R}^{|\mathbf{nodes}(t+1)|} \to \mathbb{R}^{|\mathbf{nodes}(t)|}$ is defined as

$$\rho_{|t}[J_{t+1}] = \left(\rho^i\left[J^{[i]}\right]\right)_{i \in \mathbf{nodes}(t)}. \tag{16}$$

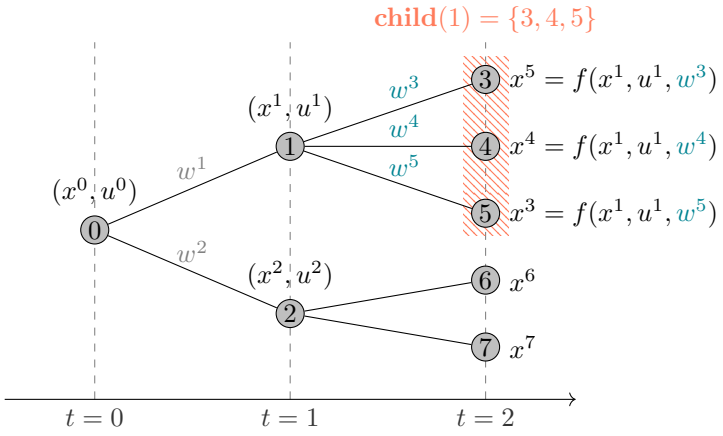

Fig. 2. Scenario tree evolution, adapted from Sopasakis et al. (2019)

The risk-averse, risk constrained optimal control problem (RAOCP) can be cast into a nested multistage formulation as (Sopasakis et al., 2019; Shapiro et al., 2014, Ch. 6)

$$\min_{u_0} J_0 + \rho_{|0}\Bigg[\min_{u_1} J_1 + \rho_{|1}\Bigg[\min_{u_2} J_2 + \dots + \rho_{|N-2}\Big[\min_{u_{N-1}} J_{N-1} + \rho_{|N-1}\big[J_N\big]\Big]\dots\Bigg]\Bigg] \tag{17}$$

subject to,

$$x_{t+1} = f(x_t, u_t, w_t), \qquad \forall t \in \mathbb{N}_{0,N-1} \tag{18}$$

$$\mathrm{AV@R}_\beta[c_t(x_t, u_t, w_t)] \leq 0. \tag{19}$$

Here, Eq. (19) is an AV@R-type risk constraint. $\mathrm{AV@R}_\beta$ serves as the convex and conservative approximation of the chance constraint $\mathrm{P}[\mathrm{c_t} > 0] \leq \beta$ (Shapiro et al., 2014, Ch. 6). This stagewise risk constraint fails to describe how the ambiguity fails to propagate in time. To incorporate the evolution of ambiguity, multistage nested risk constraints can be imposed (Sopasakis et al., 2019).

2.5 Tractable reformulation

The tractable reformulation of the RAOCP is based on the conic representation of coherent risk measures and epigraphical relaxations. The ambiguity set of a coherent risk measure can be cast into a conic inequality with the matrices E, F and a vector b such that

$$\rho[Z] = \max_{\mu\in\mathbb{R}^n, \nu\in\mathbb{R}^r} \Big\{\mu^\top Z \mid E\mu + F\nu \preccurlyeq_{\mathcal{K}} b\Big\}, \tag{20}$$

where $\mathcal{K}$ is a closed convex cone. Furthermore, when strong duality holds (i.e., if there exists μ^*, v^* such that, $b - E\mu^* + Fv^* \in \mathbf{ri}(\mathcal{K})$ (Ben-Tal and Nemirovski, 2001) [1]), the risk measure can be written as

$$\rho[Z] = \min_y \{y^\top b \mid E^\top y = Z, F^\top y = 0, y \succcurlyeq_{\mathcal{K}^*} 0\}. \tag{21}$$

For $\mathrm{AV@R}_\alpha$, $E = [1_n^\top \quad -1_n^\top \quad \alpha\mathbb{I}_n \quad -\mathbb{I}_n]^\top$, $F = 0$, $b = [1 \quad -1 \quad \pi \quad 0_n]^\top$, and $\mathcal{K} = \mathbb{R}^{2n}_{\geq 0}$.

The epigraph of a coherent risk measure ρ, i.e., the set $\mathbf{epi}\,\rho = \{(Y, \gamma) \in \mathbb{R}^{n+1} \mid \rho[Y] \leq \gamma\}$, is given by

$$\mathbf{epi}\,\rho = \left\{(Y,\gamma) \in \mathbb{R}^{n+1} \;\middle|\; \begin{array}{l} \exists y \succcurlyeq_{\mathcal{K}^*} 0, E^\top y = Y \\ F^\top y = 0, y^\top b \leq \gamma \end{array}\right\}. \tag{22}$$

[1] $\mathbf{ri}(\mathcal{K})$ is the relative interior of $\mathcal{K}$

The epigraph of a conditional risk measure is the Cartesian product of the epigraphs of the underlying risk measures.

With help of the risk-infimum interchangeability property (Sopasakis et al., 2019, Th 5.1), the problem in Eq. (17) can be cast as

$$\underset{u_0, u_1 \dots, u_{N-1}}{\mathbf{minimize}}\; J_0 + \rho_{|0}\Big[J_1 + \rho_{|1}\Big[J_2 + \dots + \rho_{|N-1}\big[J_N\big]\dots\Big]\Big]. \tag{23}$$

This is equivalent to

$$\underset{\substack{u_0,u_1,\dots,u_{N-1}\\ \tau_0,\tau_1,\dots,\tau_N}}{\mathbf{minimize}}\; \tau_0 + \rho_{|0}\Big[\tau_1 + \rho_{|1}\Big[\tau_2 + \dots + \rho_{|N-1}\big[\tau_N\big]\dots\Big]\Big] \quad \text{subject to,} \quad J_t \leq \tau_t, \quad t \in \mathbb{N}_{[0,N]}, \tag{24}$$

where $\tau_t \in \mathbb{R}^{|\mathbf{nodes}(t)|}$. The epigraphical relaxation then follows from the innermost risk mapping which is written as

$$\rho_{|N-1}\big[\tau_N\big] = \inf\{s_{N-1} \mid (\tau_N, s_{N-1}) \in \mathbf{epi}\,\rho_{|N-1}\}. \tag{25}$$

Eq. (24) then becomes,

$$\begin{aligned} \underset{\substack{u_0,u_1,\dots,u_{N-1}\\ \tau_1,\tau_2,\dots,\tau_N,s_{N-1}}}{\mathbf{minimize}} \quad & \tau_0 + \rho_{|0}\Big[\tau_1 + \rho_{|1}\Big[\tau_2 + \dots \\ & \qquad + \rho_{|N-2}\big[\tau_{N-1} + s_{N-1}\big]\dots\Big]\Big] \\ \text{subject to,} \quad & J_t \leq \tau_t, \quad t \in \mathbb{N}_{[0,N]} \\ & (\tau_N, s_{N-1}) \in \mathbf{epi}\,\rho_{|N-1}. \end{aligned} \tag{26}$$

Similarly relaxing the innermost risk mappings recursively leads to the following optimisation problem

$$\begin{aligned} \underset{\substack{u_0,u_1,\dots,u_{N-1}\\ \tau_1,\tau_2,\dots,\tau_N\\ s_0,s_1,\dots,s_N}}{\mathbf{minimize}} \quad & \tau_0 + s_0 \\ \text{subject to,} \quad & J_t \leq \tau_t, \quad t \in \mathbb{N}_{[0,N]} \\ & (\tau_{t+1} + s_{t+1}, s_t) \in \mathbf{epi}\,\rho_{|t}, \quad t \in \mathbb{N}_{[0,N-1]}, \\ & s_N = 0 \end{aligned} \tag{27}$$

As we use $\mathrm{AV@R}_\alpha$ as the risk measure (which can be described by the tuple $(E^i, b^i, \mathcal{K}^i)$) at every node, the problem in Eq. (17) can be replaced by

Table 2. Mean final product concentration with changing values of α for the AV@R$_\alpha$ objective and AV@R$_\beta$ risk constraint $\beta = 0.5$

Objective α	Final product concentration (g/L)
0	1.6679
0.2	1.6679
0.4	1.6682
0.6	1.6712
0.8	1.6714
1.0	1.6718

$$\begin{aligned} \underset{\substack{u_0,u_1,\ldots,u_{N-1}\\ \tau_1,\tau_2,\ldots,\tau_N\\ s_0,s_1,\ldots,s_N}}{\textbf{minimize}} \quad & \tau_0 + s_0 \\ \text{subject to,} \quad & x^0 = x_0 \text{ and } x^{i+} = f(x^i, u^i, w^{i+}), \\ & y^i \preccurlyeq_{(\mathcal{K}^i)^*} 0,\ (E^i)^\top y^i = \tau^{[i]} + s^{[i]}, \\ & (y^i)^\top b \le s^i, \\ & J_t \le \tau_t \\ & s_N = 0. \end{aligned} \tag{28}$$

where $t \in \mathbb{N}_{[0,N-1]}$, $i \in \textbf{nodes}(t)$ and $i_+ \in \textbf{child}(i)$. Similarly, the stage wise risk constraints can be reformulated as $(c_t, 0) \in \textbf{epi}\, \hat{\rho}_t)$. For AV@R$_\beta$ type risk constraints (described by tuple $(\hat{E}^i, \hat{b}^i, \hat{\mathcal{K}}^i)$), the epigraphical relaxation leads to

$$\hat{y}_t \preccurlyeq_{(\hat{\mathcal{K}}_t)^*} 0, \quad \hat{E}_t^\top \hat{y}_t = \eta_t, \tag{29}$$

$$\hat{y}_t^\top \hat{b}_t \le 0, \qquad c_t(x^i, u^i) \le \eta_t^i, \tag{30}$$

with $i \in \textbf{nodes}(t)$ and additional variables $\eta_t \in \mathbb{R}^{|\textbf{nodes}(t)|}$.

The final dynamic optimisation problem is solved recursively in an MPC framework. A 30 stage prediction horizon is considered along with a 3 stage robust horizon. The robust horizon indicates how far the scenario tree branches. In this case, after three stages the tree stops branching , i.e., $w_t = w_{\min(t,3)}$. This helps avoid extensive computational times. The dynamic system described in Eq. (1) - Eq. (4) is discretised using an explicit Euler scheme. The problem is solved in MATLAB using two toolboxes. `Marietta`[2] is used to generate scenario trees and assign probabilities to each node. The scenario tree is generating using the values $S_{in} \in \{150, 200, 250\}$ with probabilities $\pi = [0.25,\ 0.5,\ 0.25]^\top$. The process model considers S_{in} varying every hour following a normal distribution. Although `Marietta` can be used to construct and solve risk-averse problems using YALMIP, in this work `CasADi` (Andersson et al., 2019) is used. Within `CasADi`, the optimisation problem is solved using the interior point method as available through IPOPT.

3. RESULTS

Figure 3 depicts the performance of RAMPC for 100 Monte Carlo simulations with uncertain S_{in}. This figure depicts the case with objective $\alpha = 0.4$, and constraint $\alpha = 0.5$. The control and state profile resemble the analytical solution. Furthermore, in the 100 simulations performed, the constraints were violated only in 9 cases. The mean of the maximum product concentration obtained at the end from the 100 simulations is 1.6712 g/L. This is slightly lower than the 1.68 g/L product obtained via the analytical solution. However, the analytical solution does not consider the influence of uncertainty.

[2] Available at: `https://github.com/kul-optec/risk-averse`

Table 3. Mean final product concentration with changing values of β for the AV@R$_\beta$ risk constraint and AV@R$_\alpha$ objective $\alpha = 0.5$

Risk Constraint β	Final product concentration (g/L)
0.0	1.6672
0.2	1.6669
0.4	1.6712
0.6	1.6691
0.8	1.6703
1.0	1.6719

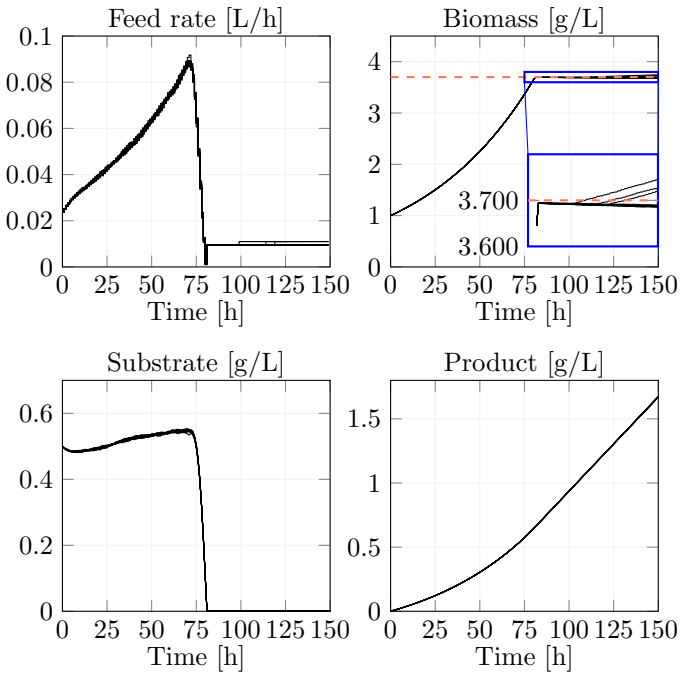

Fig. 3. Risk averse model predictive control with AV@R$_\alpha$ objective, and AV@R$_\beta$ risk constraints. The objective, $\alpha = 0.4$ and for the constraints $\beta = 0.5$. The figure depicts results of 100 Monte Carlo simulations. The state constraint was violated only in 9 cases out of the 100.

In Table 2, the final product concentrations obtained for different combinations of α values for the AV@R objective are reported. It can be seen that increasing the α value, i.e., moving from worst case scenario to risk-neutral scenario, the final optimised product concentration increases slightly.

Similarly, in Table 3, the final product concentrations obtained for different combinations of β values for the AV@R risk constraint are reported. In this case, no trend can be noticed in the optimised final product concentration with increasing β.

4. CONCLUSIONS

In this paper, a risk-averse, risk constrained formulation for the optimisation of bioreactors in an MPC framework is presented. The dynamic optimisation problem that needs to be solved at every measurement time is formulated with nested AV@R risk objective and the probabilistic chance constraints are over-approximated by AV@R type risk constraints. The formulation is rendered tractable by utilising conic dualities for coherent risk measures, and epigraphical relaxations. Future work will focus on ensuring the recursive feasibility of the MPC formulation and incorporating parametric uncertainties which are not measured into the risk-averse, risk constrained framework.

ACKNOWLEDGEMENTS

This work was supported by KU Leuven Center-of-Excellence Optimization in Engineering (OPTEC), projects G086318N and G0B4121N of the Fund for Scientific Research Flanders (FWO), the European Commission within the framework of the Erasmus+ FOOD4S Programme (Erasmus Mundus Joint Master Degree in Food Systems Engineering, Technology and Business 619864-EPP-1-2020-1-BE-EPPKA1-JMD-MOB) and by the European Union's Horizon 2020 Research and Innovation programme under the Marie Skłodowska-Curie Grant Agreement N956126 (E-MUSE Complex microbial Ecosystems MUltiScale modElling) and 813329 (PROTECT Predictive mOdelling Tools to evaluate the Effects of Climate change on food safeTy and spoilage).

REFERENCES

Alfenore, S., Cameleyre, X., Benbadis, L., Bideaux, C., Uribelarrea, J.L., Goma, G., Molina-Jouve, C., and Guillouet, S.E. (2004). Aeration strategy: a need for very high ethanol performance in saccharomyces cerevisiae fed-batch process. *Appl Microbiol Biotechnol*, 63(5), 537–542.

Andersson, J.A.E., Gillis, J., Horn, G., Rawlings, J.B., and Diehl, M. (2019). CasADi – A software framework for nonlinear optimization and optimal control. *Mathematical Programming Computation*, 11(1), 1–36.

Angeli, D., Amrit, R., and Rawlings, J.B. (2012). On Average Performance and Stability of Economic Model Predictive Control. *IEEE Transactions on Automatic Control*, 57(7), 1615–1626.

Ashoori, A., Moshiri, B., Khaki-Sedigh, A., and Bakhtiari, M.R. (2009). Optimal control of a nonlinear fed-batch fermentation process using model predictive approach. *Journal of Process Control*, 19(7), 1162–1173.

Bastin, G. (1990). *On-line estimation and adaptive control of bioreactors*. Elsevier, Amsterdam New York.

Ben-Tal, A. and Nemirovski, A. (2001). *Lectures on Modern Convex Optimization*. MOS-SIAM Series on Optimization. Society for Industrial and Applied Mathematics.

Bhonsale, S.S., De Buck, V., Joseph, J.A., and Van Impe, J. (2019). Optimal control of beer fermentation process using pomodoro. In *Proceedings of Specialized Conference on Sustainable Viticulture, Winery Wastes & Agro-industrial Wastewater Management*. University of Mons.

Çalık, P., Bayraktar, E., İnankur, B., Soyaslan, E.Ş., Şahin, M., Taşpınar, H., Açık, E., Yılmaz, R., and Özdamar, T.H. (2010). Influence of pH on recombinant human growth hormone production by pichia pastoris. *J Chem Technol Biotechnol*, 85(12), 1628–1635.

Cereghino, G.P., Cereghino, J.L., Ilgen, C., and Cregg, J.M. (2002). Production of recombinant proteins in fermenter cultures of the yeast pichia pastoris. *Curr Opin Biotechnol*, 13(4), 329–332.

Chang, L., Liu, X., and Henson, M.A. (2016). Nonlinear model predictive control of fed-batch fermentations using dynamic flux balance models. *Journal of Process Control*, 42, 137–149.

Herceg, D. (2019). *Stochastic Model Predictive Control of Nonlinear and Uncertain Systems*. Ph.D. thesis, IMT Schoot of Advanced Studies, Lucca, Italy.

Joseph, J.A., Akkermans, S., Nimmegeers, P., and Van Impe, J.F.M. (2019). Bioproduction of the recombinant sweet protein thaumatin: Current state of the art and perspectives. *Front Microbiol*, 10.

Lauwers, J., Appels, L., Thompson, I.P., Degrève, J., Van Impe, J.F., and Dewil, R. (2013). Mathematical modelling of anaerobic digestion of biomass and waste: Power and limitations. 39(4), 383–402.

Lucia, S. and Engell, S. (2013). Robust nonlinear model predictive control of a batch bioreactor using multi-stage stochastic programming. In *2013 European Control Conference (ECC)*, 4124–4129.

Mesbah, A. (2016). Stochastic Model Predictive Control: An Overview and Perspectives for Future Research. *IEEE Control Systems Magazine*, 36(6), 30–44.

Nemirovski, A. and Shapiro, A. (2007). Convex approximations of chance constrained programs. *SIAM J Optim*, 17(4), 969–996.

Nimmegeers, P., Vercammen, D., Bhonsale, S., Logist, F., and Van Impe , J. (2021). Metabolic Reaction Network-Based Model Predictive Control of Bioprocesses. *Applied Sciences*, 11(20), 9532.

Pushpavanam, S., Rao, S., and Khan, I. (1999). Optimization of a biochemical fed-batch reactor using sequential quadratic programming. *Ind Eng Chem Res*, 38(5), 1998–2004.

Rahimian, H. and Mehrotra, S. (2019). Distributionally robust optimization: A review. doi:arxiv.org/abs/1908.05659.

Rawlings, J., Mayne, D., and Diehl, M. (2020). *Model predictive control : theory, computation, and design*. Nob Hill Publishing, Santa Barbara, California.

Shapiro, A., Dentcheva, D., and Ruszczy?ski, A. (2014). *Lectures on Stochastic Programming: Modeling and Theory, Second Edition*. MOS-SIAM Series on Optimization. Society for Industrial and Applied Mathematics.

Sopasakis, P., Schuurmans, M., and Patrinos, P. (2019). Risk-averse risk-constrained optimal control. doi:arxiv.org/abs/1903.06749. URL `https://arxiv.org/abs/1903.06749`.

Srinivasan, B., Bonvin, D., Visser, E., and Palanki, S. (2003). Dynamic optimization of batch processes: II. Role of measurements in handling uncertainty. *Computers & Chemical Engineering*, 27(1), 27–44.